# Peptide conjugated chitosan foam as a novel approach for capture-purification and rapid detection of hapten - Example of ochratoxin A

R. Soleri, H. Demey, S. A. Tria, A. Guiseppi-Elie, A. I. B. N. Had Hassine, C. Gonzalez, I. Bazin

# Peptide conjugated chitosan foam as a novel approach for capture-purification and rapid detection of hapten – Example of ochratoxin A

R. Soleri [a], H. Demey [a], S.A. Tria [a], A. Guiseppi-Elie [b], A. IBN Had Hassine [a], C. Gonzalez [a], I. Bazin [a,*]

[a] Ecole des mines d'Alès, LGEI, 6 avenue de Clavière, 30319 Alès Cedex, France
[b] Clemson University, C3B, 100 Technology Drive, Clemson, SC 29634, USA

A B S T R A C T

A novel bioassay for the detection and monitoring of Ochratoxin A (OTA), a natural carcinogenic mycotoxin produced by Aspergillus and Penicillium fungi, has been developed and applied for the screening of red wine. Here we report the immobilization and orientation of NOF4, a synthetic peptide, onto 3-D porous chitosan supports using a N-terminal histidine tag to allow binding to $M^{++}$ ions that were previously adsorbed onto the high surface area biopolymer. Three divalent cations ($M^{++}=Zn^{++}, Co^{++}, Ni^{++}$) were evaluated and were found to adsorb via a Langmuir model and to have binding capacities in the order $Zn^{++} > Co^{++} > Ni^{++}$. Following $Zn^{++}$ saturation and washing, C-terminus vs. the N-terminus His-tagged NOF4 was evaluated. At 1000 μg $L^{-1}$ OTA the N-terminus immobilization was more efficient (2.5 times) in the capture of OTA. HRP labeled OTA was added to the antigen solutions (standards or samples) and together competitively incubated on biospecific chitosan foam. The chemiluminescence substrate luminol was then added and after 5 min of enzymatic reaction, light emission signals ($\lambda_{max}=425$ nm) were analyzed. Calibration curves of $\%B/B_0$ vs. OTA concentration in PBS showed that half-inhibition occurred at 1.17 μg $L^{-1}$, allowing a range of discrimination of 0.25 and 25 μ g $L^{-1}$. In red wine, the minimum concentration of OTA that the system can detect was 0.5 μg $L^{-1}$ and could detect up to 5 μg $L^{-1}$. Assay validation was performed against immunoaffinity column (IAC) tandem reversed-phase high pressure liquid chromatography with fluorescence detection (HPLC–FLD) and provided quite good agreement. The association of chitosan foam and specific peptide represents a new approach with potential for both purification–concentration and detection of small molecules. In the future this assay will be implemented in a solid-sate bioelectronic format.

*Keywords:*
Ochratoxin A
Immunoassay
Chitosan
Peptides
NOF4
Wine

## 1. Introduction

Haptens are low molecular weight chemicals that comprise a major percentage of the universe of pesticides, herbicides, toxins, metals or allergens. Haptens then are small molecules that can elicit an immune response only when attached to a large carrier such as a protein; the carrier may be one that, by itself, also does not elicit an immune response. Therefore, it is very difficult to obtain affine antibodies to such molecules. Moreover, there has been increasing demands for ultrasensitive detection for these small target analytes that can potentially induce disease. This mycotoxin, Ochratoxin A, (a secondary fungal metabolite produced mainly by several *Aspergillus ochraceus* and *Penicillium verrucosum*) is a powerful nephrotoxic, teratogenic, immunosuppressive agent that has been implicated as an endocrine disruptor as well as a contributor to increased cancer risk. The International Agency for Research on Cancer (IARC) has classified OTA in Group 2B (possibly carcinogenic agent). OTA is mainly found in improperly stored foods such as cereals, dried fruit, nuts, and beverages such as beers and wine (Blesa et al., 2004a; Varga and Kozakiewicz, 2006; Zimmerli and Dick, 1995). Several authors have already reviewed wine contamination by OTA (Blesa et al., 2004b; Varga and Kozakiewicz, 2006). Wine is a major source of daily OTA intake for the population as it is widely consumed (Jørgensen, 2005). A level of 2 μg $kg^{-1}$ of OTA in wines has been established by the Regulatory Commission of the European Community (European Commission Commission Regulation, 2005; European Commission Regulation, 2010).

There is a standardized method for the determination of this mycotoxin in food matrices(Lerda, 2011); however, food and beverage producers are constantly looking for simple, less expensive and faster bioanalytical solutions. Indeed, validated standard methods for the detection of OTA are based on chromatographic

* Corresponding author.
*E-mail address:* ingrid.bazin@mines-ales.fr (I. Bazin).

techniques with fluorescence detection due to the fact that OTA possesses natural fluorescence (Sofie et al., 2010; Tessini et al., 2010; Aresta et al., 2006; Visconti et al., 1999). However, recent studies have proposed new lower cost assays with higher rapidity and sensitivity compared to the methods already on the market (Nasir and Pumera, 2014). These assays belong to three broad classes of analytical techniques: enzyme linked immunosorbent assays (ELISAs), test strips and biosensors.

First, OTA detection has been widely done by competitive ELISA in the past few years. Morgan et al. (1986), reported an assay in barley. Later, the sensitivity of this assay in barley samples was ca. 5 $\mu g\ kg^{-1}$ (Ramakrishna et al., 1990). Second, immunochromatographic strip (ICS) or the test strip, also called lateral flow device based on immobilized antibodies on a membrane, has also been used for the detection of OTA. These are semi-quantitative and give faster results (2–15 min) than ELISA assays (ca. 30–40 min). Test strips display different visual limits of detection (LOD) as a function of the nature of the sample (Krska and Molinelli, 2009; Shim et al., 2009). The LOD was initially set at ca. 500 $\mu g\ L^{-1}$ of OTA (Cho et al., 2005; Rusanova et al., 2009), but, nowadays, the Food and Drugs Administration has allowed a maximum of 1 $\mu g\ L^{-1}$, so the cutoff level was dropped down this the lower limit. Finally, immuno-biosensors are the last technique used to detect OTA in various samples, but their efficiency depends of the nature of the bioreceptor and biotransducer. A variety of immuno-biosensors were developed (e.g. electrochemical, impedimetric or conductimetric immunosensors) against mycotoxins like OTA (Alarcón et al., 2006; Liu et al., 2009; Prieto-Simón et al., 2008; Radi et al., 2009a, 2009b). Indeed, antibodies show high selectivity and affinity towards mycotoxins and so are configured into immuno-biosensors.

The use of antibodies in a detection system has some advantages (high affinity and selectivity) but also several major disadvantages depending the different sample matrix or experimental conditions of the assay. Among the disadvantages are denaturation and loss of structure-based activity in organic solvents, elevated temperatures or increased ionic strength. To overcome these drawbacks, diverse strategies have emerged. Alternatives to the use of OTA antibodies are being developed, including molecularly imprinted polymers (MIP) (Ali et al., 2010; Yu and Lai, 2010), peptides from phage display libraries (Giraudi et al., 2007) and DNA aptamers (Cruz-Aguado and Penner, 2008a, 2008b). DNA aptamers and synthetic receptor(s) (MIP) have some advantages compared to antibodies for the recognition of target molecules (He et al., 2013, 2012; Ma et al., 2013). We previously introduced a novel approach based on a peptide-based enzyme-linked immunosorbent assay (peptide-based ELISA) (Bazin et al., 2013). We have shown that the NF04 peptide allowed the detection of OTA in red wine in a sensitive manner. The use of peptides for the development of biosensors offers a number of attractive benefits. Peptides represent the simplest biological recognition elements for binding of some small molecules. There are examples of highly selective metal-binding peptide motifs available from the protein literature (Chow et al., 2005), for the recognition of OTA (Giraudi et al., 2007) and very recently for the binding of BPA (Yang et al., 2014). Chitosan is the second most abundant biopolymer on Earth and its ability in the sorption of divalent metal ions from aqueous solutions has been widely demonstrated; different authors have reported that chitosan is an effective low-cost sorbent due to its easy availability (Demey et al., 2014).

In the present study, we report a new bioanalytical format for the peptide-based ELISA assay. This new format allows the rapid capture, concentration and detection of hapten molecules such as OTA using NOF4. (Fig. SM1, Supplemental materials). The histidine tagged labeled peptide was immobilized and oriented on chitosan foam through adsorbed divalent zinc ions. Following washing step, OTA–HRP conjugate was added to antigen containing buffer solutions or wine samples and chemiluminescence was measured. As this approach is a based on a competitive ELISA format, the concentration of antigen is inversely proportional to the chemiluminescence light intensity measured.

## 2. Material and methods

### 2.1. Materials and chemicals

Solutions of metal ions were prepared from $ZnSO_4 \cdot 6H_2O$; $CoCl_2 \cdot 6H_2O$ and $Ni(NO_3)_2 \cdot 6H_2O$ reagents provided by Panreac (France). Chitosan was supplied by Aber Technologies (France) and its molecular weight (125,000 $g\ mol^{-1}$) determined using size exclusion chromatography (SEC) coupled with light scattering and refractometry was previously reported (Ruiz et al., 2001). The degree of deacetylation, determined by Fourier Transform infrared (FTIR) spectroscopy, was found to be 87% (Guibal et al., 1999). OTA was obtained from Sigma-Aldrich (France) from which a solution was prepared (1 $mg\ ml^{-1}$) in methanol at RT. Polyethylene glycol (PEG8000) and polyvinylpolypyrrolidone (PVPP) were obtained from Promega (France). Luminol was obtained from Pierce (France) and the peptide, NFO4, was synthetized by Smartox (France).

### 2.2. Preparation of chitosan adsorbent and chitosan foam

Chitosan foam, which served as a support for the immobilized NOF4 peptide, was prepared by dissolving chitosan to a final concentration of 2% (w/w) in 2% aqueous acetic acid solution under continuous agitation. The solution was poured into cylindrical molds (6 mm diameter/ height varies from 1 mm to 10 mm) and frozen for 3 h at 193 K. Then, the frozen solution was freeze-dried during 24 h (using a freeze-dryer Fisher Bioblock Scientific, France) at 223 K and 0.01 mbar. The resulting foam was put in contact with 1 M NaOH solution for 4 h and then was rinsed sequentially with 98% (w/w) and 50% (w/w) ethanol/water solution until pH 7. The resulting chitosan foam was used as sorbent of divalent metal ions ($Zn^{+2}$, $Ni^{+2}$, $Co^{+2}$).

### 2.3. Equilibrium sorption

In this work, the effectiveness of the chitosan foam to serve as a support for the immobilization of NOF4 via chelation with divalent metal ions was evaluated. In order to provide a material that was easy to handle, the metal ions $Zn^{+2}$, $Co^{+2}$ and $Ni^{+2}$ were separately introduced to the polymeric matrix of chitosan using a batch sorption system. The ability of chitosan to strongly interact with divalent metal ions through primary amine groups is well documented (Wan et al., 2010). Mono-component isotherms were obtained by mixing 0.2 g of sorbent (chitosan foam) at room temperature (20 °C) with a constant volume (0.2 L) of aqueous metal ion solution ($Zn^{+2}$, $Co^{+2}$ and $Ni^{+2}$) at different concentrations (ranging from 50 to 6000 $mg\ L^{-1}$). The pH of the solutions was adjusted to 5.0 with a buffer solution (consisting of sodium acetate). After 72 h of agitation, the residual metals concentration was analyzed with an Inductively Coupled Plasma Atomic Emission Spectrometer ICP-AES (HORIBA JOBIN YVON, France) at the wavelength 221.6 nm for $Ni^{+2}$, 238.8 nm for $Co^{+2}$, and 213.8 nm for $Zn^{+2}$.

The Langmuir and Freundlich models were used to describe the experimental adsorption isotherm data. These models are represented by the following equations, respectively (Freundlich, 1906; Langmuir, 1918):

$$q = \frac{q_{max}\, bCe}{1 + bCe}(1)$$

$$q = K_F C_e^{1/n} \quad (2)$$

where $q$ is the amount of metal adsorbed per gram of sorbent at equilibrium (mg $g-^{1}$), $q_{max}$ is the maximum adsorption capacity of the adsorbent (mg $g^{-1}$), and $C_e$ is the equilibrium concentration of the solution (mg $L^{-1}$). In the Langmuir model (Eq. (1)), $b$ is related to the energy of adsorption (L $mg^{-1}$), whereas $K_F$ and $n$ are the Freundlich adsorption constants, indicative of the relative capacity and the adsorption intensity, respectively.

### 2.4. Influence of contact time

The uptake kinetics experiment was performed by adding (under continuous stirring) a known amount of adsorbent (i.e., 0.2 g) to 200 mL of aqueous metal ion solution (200 mg $L^{-1}$,600 mg $L^{-1}$ and 900 mg $L^{-1}$) at pH 5. Aliquots of adsorbate (aqueous metal ion solution) were withdrawn at different times and filtered after 120 h of contact. The residual concentration was determined by ICP-AES. The kinetic profiles were compared for sorption of $Ni^{+2}$ and $Zn^{+2}$ ions. The intraparticle diffusion equation (Namasivayam and Yamuna, 1995) and the pseudo-first and pseudo-second order model were applied to fit the experimental data. These models are frequently used to describe the batch sorption system:

Pseudo-first order rate equation (PFORE) (Lagergreen, 1898):

$$\frac{dq_t}{d_t} = K_1(q_1 - q_t) \quad (3)$$

Integrating for the boundary conditions $t=0$ to $t=t$ and $q_t = 0$ to $q_t=q_t$:

$$\log(q_{eq} - q_t) = \log(q_{eq}) - \frac{K_1}{2.303}t \quad (4)$$

Pseudo-second order rate equation (PSORE) (Ho and McKay, 1998):

$$\frac{dq_t}{(q_{eq} - q_t)^2} = K_2 d_t \quad (5)$$

Integrating for the boundary conditions $t=0$ to $t=t$ and $q_t = 0$ to $q_t=q_t$:

$$\frac{1}{q_t} = \frac{1}{K_2 q_{eq}^2} + \frac{1}{q_{eq}}t \quad (6)$$

where $q_{eq}$ is the equilibrium sorption capacity (mg $g^{-1}$), $q_t$ is the sorption capacity (mg $g^{-1}$) at any time $t$ (h) and $k_2$ is the pseudo-second order rate constant (g $mg^{-1}$ $h^{-1}$).The parameters $q_{eq}$ and $k_2$ are pseudo-constants depending on the experimental conditions.

The intraparticle diffusion equation is (Namasivayam and Yamuna, 1995)

$$q_t = K_p t^{1/2} + C \quad (7)$$

where $C$ is the intercept, and $K_p$ is the intraparticle diffusion rate constant.

### 2.5. Peptide-based competitive enzyme-linked immunosorbent assay (peptide-based competitive ELISA) on chitosan foam

After washing with PBS, foam supports were placed in zinc solution overnight at 20 °C. Foam were then coated with the synthetic peptide NFO4 in azide containing carbonate buffered (15 mM $Na_2CO_3$, 35 mM $NaHCO_3$, 0.2 g $L^{-1}$ $NaN_3$, pH 9.6) and were incubated in 96-well plates at 37 °C for 3 h. Non-specific binding sites of the peptide-coated foam were blocked with casein solution at room temperature (RT) for 3 h before performing the immobilization. OTA–HRP (horseradish peroxidase) conjugate was added to each well in combination with phosphate buffer saline (control) or red wine sample supplemented with unlabeled OTA. The reaction was left for 30 min at 4 °C. After washing unbound OTA, 40 µl of luminol–hydrogen peroxide (Pierce, France) substrate was added to each well. After 5 min of enzymatic reaction, light emission signals ($\lambda_{max}$=425 nm) were analyzed using an automated microplate luminescence reader (Berthold, France). Light intensity was expressed in Relative Luminescent Unit (RLU). The results obtained were inversely proportional to the concentration of unlabeled OTA. During each test, nonspecific binding (negative control) was determined by using an incubation mixture (OTA–HRP) in which the peptide NFO4 was replaced by 100 µL of PBS buffer. Total analysis time per sample was ca. 40 min. All the samples were tested in triplicate and the mean of the peak light emission was taken as the final light signal value. Each point is the average ± standard deviation of three independent assays each with 4 measurements.

### 2.6. Calculation methods

In order to evaluate the peptide-based competitive assay, a calibration curve was established by using solutions containing well-defined concentrations of OTA. In direct competitive peptide-based ELISA, results are expressed in $B/B_0$ dose logarithmic function. $B$ and $B_0$ represent the enzyme-bound activity measured in the presence or absence of competitor, respectively. The standard curve was traced by plotting standard concentrations on $x$-axis (logarithmic scale) and percentage of maximal binding (express in % of $B/B_0$) on $y$-axis ($B/B_0=f$ (log [OTA])). The binding values were obtained by dividing the light intensity of each testing well $B$ (the luminescence measured when OTA–HRP and unlabeled OTA are in competition with NFO4 peptide) by the light intensity of the positive control well, $B_0$ (maximum luminescence obtained with OTA–HRP). This method allows the comparison of results between assays performed on different plates or on different days. While the absolute light emission may differ from plate to plate or day to day, the percentage of $B/B_0$ values are expected to be consistent from one plate to the next. All measurements were made in triplicate. A decreasing exponential function ($y=y_0+Ae^{-R0x}$) was performed on the standard curve $B/B_0=f$ (log [OTA]) by using Origin Lab software. The limit of detection (LOD) was obtain from the equation for $y=A$, the maximum with $y=y_0$ and $IC_{50}$ with $y=50$.

### 2.7. Preparation of matrix samples for peptide ELISA: wine pretreatment

In order to study matrix-associated effects, a study with red wine was carried out. A sample of 10 ml of wine supplemented (or not) with OTA (1.25 to 15 µg $L^{-1}$) (standard addition technique), was diluted with 10 mL of PEG8000 1%-$NaHCO_3$ 5% solution. This mixture was incubated for 30 min at RT on a rocker. Afterwards, it was centrifuged at 8000 rpm for 15 min. The whole sample was filtered before analysis with the peptide-based enzyme-linked immunosorbent assay.

## 3. Results and discussion

### 3.1. Equilibrium studies for metal ion adsorption

Adsorption isotherms describe the distribution of the metal ions between the liquid and the solid phases at equilibrium. Fig. 1 compares the sorption isotherms for the three candidate ions at

pH=5. The curves are characterised by the appearance of a saturation plateau at high metal ion concentration. The initial slopes are very steep, indicating that the affinity of the sorbent for metal ions is very strong. Langmuir and Freundlich models were tested. The Langmuir equation provided a better fit of the experimental data ($0.852 < R^2 < 0.959$) than did the Freundlich equation ($0.835 < R^2 < 0.952$) (Table SM1); nevertheless both models were found to adequately fit the experimental results. The removal uptake follows this order: $Zn^{+2} > Co^{+2} > Ni^{+2}$ and the maximum sorption capacity reached 230.3 mg $g^{-1}$ for $Zn^{+2}$, 87.3 mg $g^{-1}$ for $Co^{+2}$ and 62.0 mg $g^{-1}$ for $Ni^{+2}$; the molar ratio between metals and chitosan was determined as the ratio between the maximum amount of adsorbed metal (mol) and the mass of chitosan (mol) used to plot the isotherms. The corresponding value for $Zn^{+2}$, $Co^{+2}$ and $Ni^{+2}$ was found to be 440 $mol_{Zn(II)}(mol_{chitosan})^{-1}$, 185 $mol_{Co(II)}(mol_{chitosan})^{-1}$ and 132 mol $_{Ni(II)}(mol_{chitosan})^{-1}$ respectively. These results are consistent with previously reported results (Juang and Shao, 2002; Monier et al., 2010) and the sorption capacities are of the same order of magnitude.

Adsorption of heavy metals by raw and chemically modified chitosan materials has been widely studied (Guibal Milot and Tobin, 1998; Huang et al., 1996; Juang and Shao, 2002). Different processes such as adsorption, ion-exchange and chelation have been reported as the mechanisms responsible for complex formation between chitosan and metal ions; nevertheless, the type of interaction depends on the metal and on the pH of the solution (Vold et al., 2003). Ghaee et al. (2012) have reported the sorption mechanism of nickel ions on porous chitosan membrane as the combination of chelation and electrostatic adsorption; amino ($-NH_2$) and/or hydroxy groups serve as coordination sites (Wan et al., 2010). Juang and Shao (Juang and Shao, 2002) also pointed that the uptake of transition metals is performed via coordination with $-NH_2$ groups on chitosan. The possible reaction between amino groups and metal ions in this study are:

$$-NH_3^+ + Ni^{+2} \leftrightarrow NH_2Ni^{+2} + H^+ \quad (8)$$

$$-NH_3^+ + Zn^{+2} \leftrightarrow NH_2Zn^{+2} + H^+ \quad (9)$$

$$-NH_3^+ + Co^{+2} \leftrightarrow NH_2Co^{+2} + H^+ \quad (10)$$

As shown in Fig. SM2, the sorption capacity for $Zn^{+2}$ increased even at high metal concentrations; Juang and Shao (2002) attributed this increase to the possibility of a micro-precipitation of metals at the vicinity of adsorbent particles, as a result of very small change of the pH. Parameter $R_L$ (Eq. 11), defined as a dimensionless separation factor, was used by Demey et al. (2014) to determine if an isotherm is favorable or unfavorable:

$$R_L = \frac{1}{1 + b\mathrm{Co}} \quad (11)$$

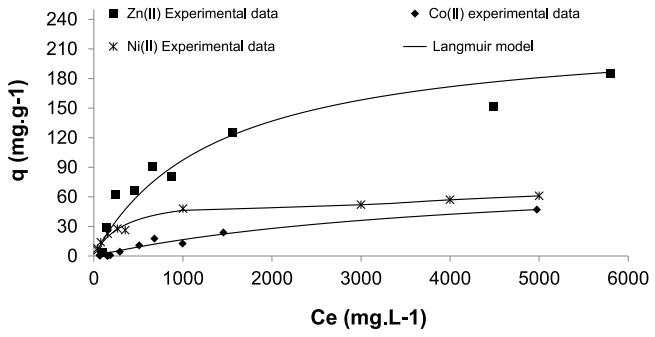


**Fig. 1.** Sorption of divalent metal ions; sorption mono-component isotherms for Zn (II), Co(II) and Ni(II).

where b is the Langmuir constant (L $mg^{-1}$). According to Öztürk and Kavak [(Oztürk and Kavak, 2005)], the value of $R_L$ characterises the shape of the isotherm: $R_L=1$ Linear; $R_L>1$ Unfavorable; $0<R_L<1$ Favorable; $R_L=0$ Irreversible. The value of $R_L$ calculated using Eq. (11) indicated that metal ion adsorption using chitosan foam is favorable (at 20 °C) for a metal ion concentration of 100 mg $L^{-1}$ (Table SM1).

### 3.2. Influence of contact time

Fig. SM2 shows the kinetic profile for the adsorption of $Zn^{+2}$ and $Ni^{+2}$ using chitosan foam as adsorbent at different initial metal concentrations; all of the plots have similar trend. Two steps can be observed; an initial fast sorption followed by a slow-rate step when approaching the equilibrium. As expected, the metal ion concentration influences the adsorption capacity at equilibrium and eventually the kinetic profile. The initial section of the kinetic profile usually governed by the resistance to ion diffusion (Demey et al., 2014) changes significantly in the case of both metals ($Zn^{+2}$ and $Ni^{+2}$); increasing the concentration, the slope of this section becomes steeper. The final section usually governed by the resistance to film diffusion (Demey et al., 2014) is also affected; sorption capacity tends to be lower with decreasing metal concentration (Table SM2). As proposed by Demey et al. (2014), this can be due to the decrease of the concentration gradient between the solution and the surface of the sorbent, and between the surface of the sorbent and the core of the sorbent. As a result, the driving force decreased as well as the sorption rate.

The experimental results can be fitted by PFORE (pseudo-first order) and PSORE (pseudo-second order) models (Table SM2); the correlation coefficients for both models are similar. Fig. SM3 shows the linear plot obtained from Eq. (7); as it can see, it does not pass through the origin, verifying that intraparticle diffusion is not the unique step that controls the metal uptake kinetics. Increasing the initial concentration of metals increases the intraparticle diffusion rate constant.

### 3.3. Specific assembly with 6His-tagged protein

Despite advances, peptide/protein assembly onto surfaces remains challenging. Here, we report a method to assemble His-tagged peptide to chitosan membrane using the divalent metal ion, $Zn^{++}$. Specific assembly with 6His-tagged protein or peptide was performed using two proteins: 6His-tagged GFP and non-His-tagged GFP. The ability to bind histidine tagged proteins was tested with various metal ions (Fig. 2). On one hand, for all divalent metal ions tested, we can see that in the presence of GFP without 6-histidine tag there is no adsorption and hence no fluorescence of the chitosan foam was observed. Interestingly, this confirms that there is little to no non-specific adsorption of proteins, such as GFP, to chitosan foam. The fluorescence level was similar to that of the negative control (chitosan saturated with divalent metals and without GFP). However, we observe a high level of fluorescence in the presence of the GFP containing a 6-histidine tag. This result is observed regardless of the metal used. But, the highest level of fluorescence was observed when the chitosan was saturated with zinc metal ions, consistent with the results obtained from isotherm calculations and loading capacity calculations. These results had been confirmed by chemiluminescence detection (on the same chitosan sorbent) by using a primary GFP antibody (rabbit) and a secondary anti-rabbit antibody HRP labeled (data not show). These data demonstrate that there exists specific biding of a 6-histidine tagged protein on chitosan foam saturated with divalent metal. The maximum sorption capacity was best for zinc metal ions and so

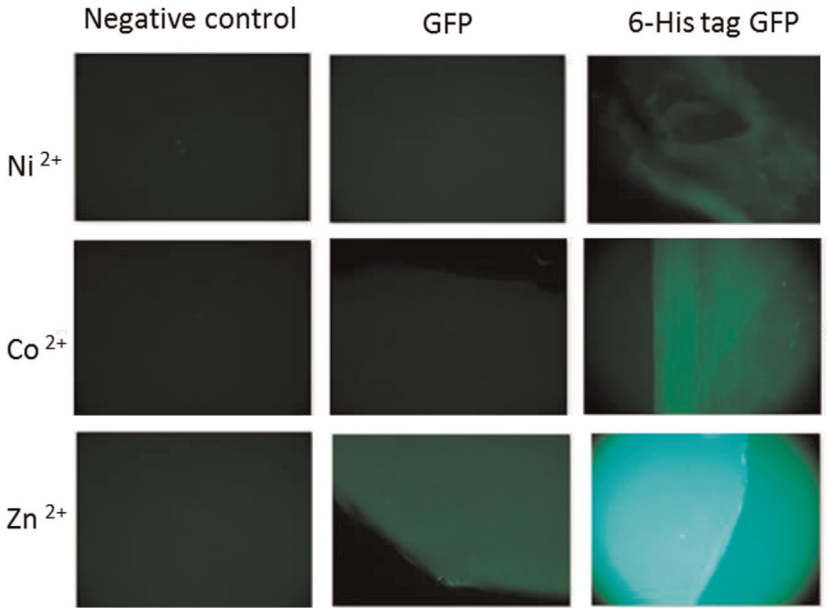


**Fig. 2.** Fluorescent microscopy images of chitosan foam.

the bidding of the 6-histidine tagged protein was likewise better with this metal ion.

### 3.4. Optimization of ochratoxin A detection

To develop a reliable tool for OTA detection based on peptide competitive ELISA, different parameters should be optimized, including the immobilized peptide orientation and concentration, the volume of chitosan foam and the dilution factor of the OTA–HRP label.

#### 3.4.1. Influence of the orientation of the peptide NFO4 on OTA–HRP detection

wFor this new approach of OTA detection, we use a peptide (NFO4), modified with and immobilized via 6-histidine tag onto $Zn^{++}$ loaded chitosan foam. The immobilization of this peptide can be achieved at the N-terminal or C-terminal extremity, leading to a binding to the OTA by the opposite extremity. To optimize the recognition of the toxin, we first tested the orientation of the peptide on the chitosan foam. The peptide was histidine tagged at the N-terminal or C-terminal extremity and immobilized through divalent zinc ion adsorbed on chitosan foam (Fig. 3a). The construct was evaluated using varying concentrations of OTA–HRP conjugate. For a concentration of 166.6 $\mu g\ L^{-1}$ we could not discriminate the control ($3600 \pm 530$ RLU) from the C-terminus ($11{,}820 \pm 6650$ RLU) and N-terminus ($25{,}440 \pm 11{,}600$ RLU) immobilized NFO4. For 250 and 500 $\mu g\ L^{-1}$, we can clearly see a difference between the control ($5220 \pm 1410$ RLU and $11{,}920 \pm 3840$ RLU) and the presence of peptide, but no difference was observed between the two peptide orientations; C-terminus ($112{,}540 \pm 40{,}460$ RLU and $97{,}540 \pm 43{,}800$ RLU) or N-terminus ($88{,}020 \pm 31{,}190$ RLU and $69{,}410 \pm 19{,}570$ RLU). While, in the case of 1000 $\mu g\ L^{-1}$ OTA–HRP conjugate, the recognition by the N terminus is close to 2.5 times that of the C-terminus (respectively $611{,}850 \pm 21{,}028$ RLU and $251{,}160 \pm 78$, 380 RLU). For all of the subsequent optimization steps, the NFO4 peptide oriented with N-terminus his-tag modification was used as the recognition element.

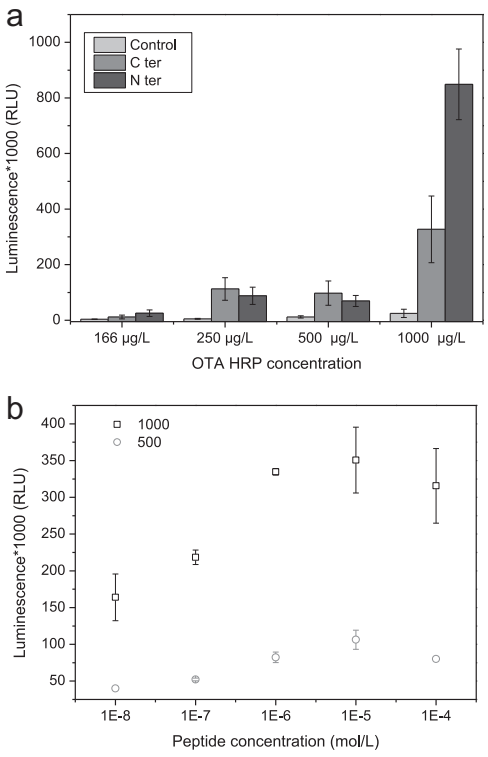


**Fig. 3.** Optimization of peptide ELISA based on chitosan foam parameters: (a) Influence of the orientation of the peptide NFO4. Peptide-based competitive ELISA assays for the detection of OTA in PBS on chitosan foam. The negative control is the luminescence emitted with OTA–HRP without NFO4 peptide. Each point are the average $\pm$ standard deviation of four assays, each of triplicate measurement ($n=12$). (b) Optimization of peptide NFO4 concentrations and OTA–HRP concentration. ELISA type assays carried out on chitosan foam for different peptide NFO4 concentration and an OTA–HRP concentration at 1000 $\mu g\ L^{-1}$ (rectangle) or 500 $\mu g\ L^{-1}$ (circle). Each point is the average $\pm$ standard deviation of three independent essays each with 4 measurement ($n=12$).

### 3.4.2. Optimization of peptide NFO4 and OTA–HRP labeled concentration.

The optimal concentration of NFO4 peptide and OTA–HRP were then determined by ELISA assay. Different concentrations of peptide were prepared in carbonate buffer and ELISA assays were carried out with a concentration of OTA HRP at 500 μg $L^{-1}$ or 1000 μg $L^{-1}$. When OTA–HRP was used at a concentration of 1000 μg $L^{-1}$, responses were always higher compared to the OTA–HRP concentration at 500 μg $L^{-1}$ and the responses obtained at different NFO4 concentrations can be clearly discriminated (Fig. 3b). However, when 500 μg $L^{-1}$ OTA HRP was used the resulting luminescence results were in the same range. Therefore, the OTA–HRP concentration at 1000 μg $L^{-1}$ was chosen for all subsequent experiments. Concerning the peptide concentration, we can see a response increase with the increase of peptide concentration up to $10^{-6}$ mol $L^{-1}$, followed by a decrease of the signal known as hook effect (Agarwal et al., 2010). In order to obtain a maximum response while avoiding the hook effect, a concentration of $10^{-6}$ mol $L^{-1}$ of peptide was chosen for subsequent experiments.

### 3.4.3. Optimization of chitosan foam volume

To develop this new detection system, we produced porous chitosan foam to serve as the immune-support. Depending on the volume used, various chitosan foams (Fig. 4a) were fabricated. With small volumes were created thick slices of chitosan foam and with larger volumes, large disks or tubes. Analysis of foams by SEM showed the developed materials to be highly porous and to present a large exchange surface. As the aim of this project was to develop reliable tools for the detection of haptens, this requires a format that can be produced on a large scale and also allow multiple measurements. For these reasons the slice format was chosen. We then investigated the effect of chitosan foam slice volume on the luminescence obtained with a peptide concentration of 10-6 μg · $L^{-1}$ and OTA–HRP concentration of 1000 μg $L^{-1}$. As shown on Fig. 4c, the use of foam ranging from 10 to 70 μL gave the same luminescence intensity while a clear increase of the signal was obtained with higher volumes ranging from 80–100 μL. To achieve a better sensitivity, foam of 100 μL are chosen for the detection of OTA in the subsequent experiments.

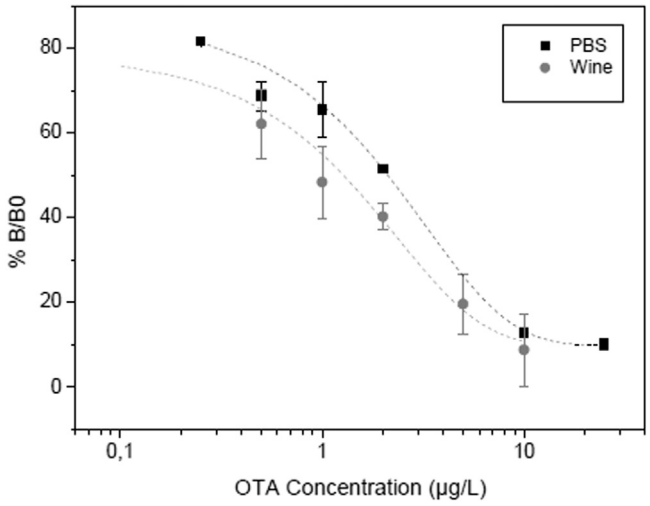


**Fig. 5.** OTA calibration curves in PBS and red wine on chitosan foam. a. Competitive ELISA for the detection of OTA in PBS were performed with a concentration of peptide NFO4 of $10^{-6}$ M for a concentration of OTA–HRP labeled at 1000 μg $L^{-1}$. *B* and $B_0$ represent the bound enzyme activity measured in the presence or absence of competitor respectively. Each point is the average ± standard deviation of three independent assays each with 4 measurement ($n=12$). b. Calibration curve in red wine for OTA spiked samples: Competitive ELISA for the detection of OTA in wine were performed with a concentration of peptide NFO4 of $10^{-6}$ M for a concentration of OTA–HRP labeled at 1000 μg $L^{-1}$ . B and $B_0$ represent the bound enzyme activity measured in the presence or absence of competitor respectively. Each point is the average ± standard deviation of three independent assays each with 4 measurement ($n=12$).

### 3.5. Direct detection of OTA in PBS

Competitive ELISAs were performed with a concentration of peptide NFO4 at $10^{-6}$ M and for a concentration of HRP-labeled OTA (OTA–HRP conjugate) at 1000 μg $L^{-1}$ using foam support slices that were formed from 100 μL of chitosan solution. The concentration of OTA was varied from well to well (0 μg $L^{-1}$, 0.25 μg $L^{-1}$, 0.5 μg $L^{-1}$, 1 μg $L^{-1}$, 2 μg $L^{-1}$, 5 μg $L^{-1}$, 10 μg $L^{-1}$ and 25 μg $L^{-1}$). The standard curves obtained for peptide-based competitive ELISA on chitosan foam in PBS are shown in Fig. 5 (squares). The competitive binding process was represented by the exponential curve fit for the standard OTA in PBS. Inhibition was observed to start at 0.25 μg $L^{-1}$.The maximum inhibition was

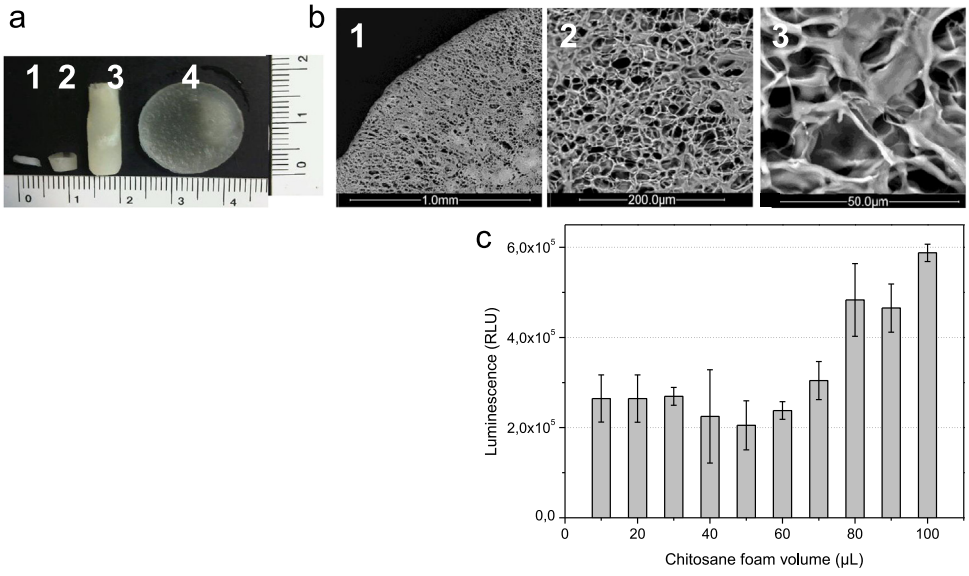


**Fig. 4.** Optimization of chitosan foam volume. a. Various production of chitosan foam. 1. foam of 30 μl; 2. foam of 100 μl, 3 and 4 foam of 1 ml: b. SEM images of chitosan foam at different magnification 1. ×50, 2. ×200 and 3. ×1000. c. Luminescence in function of chitosan foam volume with $10^{-6}$ M of peptide NFO4.

**Table 1**
Comparison test of wine sample from Inter Rhone laboratory and the peptide ELISA based on chitosan foam.

| Wine sample # | $\%B/B_0$ | OTA concentration in sample (ppb) | OTA concentration mesured (ppb) |
|---|---|---|---|
| 161 | 41.55 | 1.3 | 1.84 |
| 164 | 54.57 | 2.9 | 1.02 |
| 170 | 28.16 | 3.0 | 3.14 |
| 173 | 24.48 | 4.0 | 3.67 |
| 176 | 27.96 | 3.9 | 3.16 |
| 179 | 13.84 | 5.7 | 6.77 |
| 191 | 17.14 | 5.4 | 5.32 |

obtained at 10 $\mu g\,L^{-1}$ and half inhibition occur at 2.11 $\mu g\,L^{-1}$. Inhibition was complete, which was expected since the tracer is also OTA-based. From the calibration curve parameters, and with the SD values, the range of detection of OTA in PBS was established to be between 0.25 and 10 $\mu g\,L^{-1}$.

### 3.6. Direct detection of OTA in wine

The measurement of OTA in real-world samples and the direct comparison of these results with standard laboratory analysis procedures served to establish the efficacy of this new method. Natural red wine samples were spiked with various concentrations of OTA. These results were used for a repeat of the calibration curve (Fig. 5 (circles)) in the wine matrix. Wine containing OTA could readily be measured by the system, with a reduction in efficacy which can easily be explained by the complexity of the wine matrix and the enhanced number of non-specific compounds co-present in wine samples. The minimum concentration of OTA that the system can detect was 0.5 $\mu g\,L^{-1}$ and it can detect more than 5 $\mu g\,L^{-1}$. The current assay method was validated in a study using real wine samples from the "Domaine de Pech Rouge-11430 Gruissan, France", which are documented to naturally contain OTA and have been previously analyzed (Fabiani et al., 2010). The results of the current assay method were compared with those obtained using a reference method (Fabiani et al., 2010; Visconti et al., 1999). This method of reference has been made by Inter Rhône laboratory and used immunoaffinity column (IAC) recovery followed by reversed-phase high pressure liquid chromatography using fluorescence detection (HPLC–FLD). The results obtained (Table 1) are in generally good agreement confirming the applicability of the current assay for the successful screening of wines for OTA.

## 4. Conclusion

A novel method has been described for the immobilization of the biorecognition peptide NFO4 onto three-dimensional porous chitosan foam that was pre-adsorbed with divalent $Zn^{+2}$ ions. The porous chitosan foam was shown to adsorb divalent cations with binding capacities in the order $Zn^{+2} > Co^{+2} > Ni^{+2}$; maximum sorption capacities reached 230.3 mg $g^{-1}$ for $Zn^{+2}$, 87.3 mg $g^{-1}$ for $Co^{+2}$ and 62.0 mg $g^{-1}$ for $Ni^{+2}$. Peptides were immobilized via a histidine tag. Comparison of the efficacy of histidine tag modification and hence immobilization using the C-terminus vs. the N-terminus has revealed that at 1000 $\mu g\,L^{-1}$ OTA the N-terminus immobilization was more efficient (2.5 times) in the capture of OTA. Sequential optimization of the key process variables has established that the immobilized peptide NFO4 was best at $10^{-6}$ M for which, in competitive format, an OTA–HRP concentration of 1000 $\mu g\,L^{-1}$ should be used on a chitosan foam volume of 100 $\mu L$. Calibration of OTA detection in PBS and in wine matrix reveled some small differences reflective of the molecular complexity of wine. Validation of assay results against the reference method has provided quite good agreement consistent with the use of this peptide-based competitive bioassay technique for the successful screening of wines for OTA. In the future this assay will be implemented in a solid-sate bioelectronic format.


## Acknowledgements

AG-E acknowledges EMA for a Visiting Distinguished Professorship and ABTECH Scientific, Inc. for financial support. Special thanks go to the French National Research Agency for supporting the COMBITOX Project (ANR-11-ECOT-009-04), which has contributed to this work. Special thanks go to D. Caboulet (Institut Français de la Vigne & du Vin Pôle Rhône-Méditerranée, France) for real wine samples.


## Appendix A. Supplementary information

Supplementary data associated with this article can be found in the online version at http://dx.doi.org/10.1016/j.bios.2014.09.084.

## References


Agarwal, M., Das, A., Singh, A., 2010. High-Dose Hook Effect In Prolactin Macroadenomas: A Diagnostic Concern. doi:10.4103/0974-1208.74164.

Alarcón, S.H., Palleschi, G., Compagnone, D., Pascale, M., Visconti, A., Barna-Vetró, I., 2006. Monoclonal antibody based electrochemical immunosensor for the determination of ochratoxin A in wheat. Talanta 69, 1031–1037. http://dx.doi.org/10.1016/j.talanta.2005.12.024.

Ali, W.H., Derrien, D., Alix, F., Pérollier, C., Lépine, O., Bayoudh, S., Chapuis-Hugon, F., Pichon, V., 2010. Solid-phase extraction using molecularly imprinted polymers for selective extraction of a mycotoxin in cereals. J. Chromatogr. A 1217, 6668–6673. http://dx.doi.org/10.1016/j.chroma.2010.04.071.

Aresta, A., Vatinno, R., Palmisano, F., Zambonin, C.G., 2006. Determination of Ochratoxin A in wine at sub ng/mL levels by solid-phase microextraction coupled to liquid chromatography with fluorescence detection. J. Chromatogr. A 1115, 196–201. http://dx.doi.org/10.1016/j.chroma.2006.02.092.

Bazin, I., Andreotti, N., Hassine, A.I.H., De Waard, M., Sabatier, J.M., Gonzalez, C., 2013. Peptide binding to ochratoxin A mycotoxin: a new approach in conception of biosensors. Biosens. Bioelectron. 40, 240–246. http://dx.doi.org/10.1016/j.bios.2012.07.031.

Blesa, J., Berrada, H., Soriano, J.M., Moltó, J.C., Mañes, J., 2004a. Rapid determination of ochratoxin A in cereals and cereal products by liquid chromatography. J. Chromatogr. A 1046, 127–131. http://dx.doi.org/10.1016/j.chroma.2004.06.086.

Blesa, J., Soriano, J.M., Moltó, J.C., Mañes, J., 2004b. Concentration of ochratoxin A in wines from supermarkets and stores of Valencian Community (Spain). J. Chromatogr. A 1054, 397–401. http://dx.doi.org/10.1016/j.chroma.2004.04.058.

Cho, Y.J., Lee, D.H., Kim, D.O., Min, W.K., Bong, K.T., Lee, G.G., Seo, J.H., 2005. Production of a monoclonal antibody against ochratoxin A and its application to immunochromatographic assay. J. Agric. Food Chem. 53, 8447–8451. http://dx.doi.org/10.1021/jf051681q.

Cruz-Aguado, J.A., Penner, G., 2008a. Fluorescence polarization based displacement assay for the determination of small molecules with aptamers. Anal. Chem. 80, 8853–8855. http://dx.doi.org/10.1021/ac8017058.

Cruz-Aguado, J.A., Penner, G., 2008b. Determination of ochratoxin A with a DNA aptamer. J. Agric. Food Chem. 56, 10456–10461. http://dx.doi.org/10.1021/jf801957h.

Demey, H., Vincent, T., Ruiz, M., Sastre, A.M., Guibal, E., 2014. Development of a new chitosan/Ni(OH)2-based sorbent for boron removal. Chem. Eng. J. 244, 576–586. http://dx.doi.org/10.1016/j.cej.2014.01.052.

European Commission Commission Regulation, 2005. European Commission Commission Regulation. No. 123/2005 Brussels.

European Commission Regulation, 2010. European Commission Commission Regulation, 2010. Off. J. Eur. Union 35, 7–8.

Fabiani, A., Corzani, C., Arfelli, G., 2010. Correlation between different clean-up methods and analytical techniques performances to detect Ochratoxin A in wine. Talanta 83, 281–285. http://dx.doi.org/10.1016/j.talanta.2010.08.027.

Ghaee, A., Shariaty-Niassar, M., Barzin, J., Zarghan, A., 2012. Adsorption of copper and nickel ions on macroporous chitosan membrane: Equilibrium study. Appl. Surf. Sci. 258, 7732–7743. http://dx.doi.org/10.1016/j.apsusc.2012.04.131.

Giraudi, G., Anfossi, L., Baggiani, C., Giovannoli, C., Tozzi, C., 2007. Solid-phase extraction of ochratoxin A from wine based on a binding hexapeptide prepared

by combinatorial synthesis. J. Chromatogr. A 1175, 174–180. http://dx.doi.org/10.1016/j.chroma.2007.10.057.
Guibal Milot, C., Tobin, J.M.E., 1998. Metal-anion sorption by chitosan beads equilibrium and kinetic studies. Ind. Eng. Chem. Res. 37, 1454–1463. http://dx.doi.org/10.1021/ie9703954.
Guibal, E., Larkin, A., Vincent, T., Tobin, J.M., 1999. Chitosan sorbents for platinum sorption from dilute solutions. Ind. Eng. Chem. Res. 38, 4011–4022. http://dx.doi.org/10.1021/ie990165k.
Freundlich, H.M.F., 1906. Über die adsorption in lösungen. Z. Phys. Chem. 57, 385–470.
He, H.Z., Chan, D.S.H., Leung, C.H., Ma, D.L., 2013. G-quadruplexes for luminescent sensing and logic gates. Nucleic Acids Res. , http://dx.doi.org/10.1093/nar/gkt108.
He, H.-Z., Pui-Yan, Ma, V., Leung, K.-H., Shiu-Hin Chan, D., Yang, H., Cheng, Z., Leung, C.-H., Ma, D.-L., 2012. A label-free G-quadruplex-based switch-on fluorescence assay for the selective detection of ATP. Analyst , http://dx.doi.org/10.1039/c2an15999f.
Ho, Y.S., McKay, G., 1998. Sorption of dye from aqueous solution by peat. Chem. Eng. J. 70, 115–124. http://dx.doi.org/10.1016/S1385-8947(98)00076-X.
Huang, C., Chung, Y.C., Liou, M.R., 1996. Adsorption of Cu(II) and Ni(II) by pelletized biopolymer. J. Hazard. Mater. , http://dx.doi.org/10.1016/0304-3894(95)00096-8.
Jørgensen, K., 2005. Occurrence of ochratoxin A in commodities and processed food – a review of EU occurrence data. Food Addit. Contam. 22 (Suppl. 1), 26–30. http://dx.doi.org/10.1080/02652030500344811.
Juang, R.-S., Shao, H.-J., 2002. Effect of pH on competitive adsorption of Cu(II), Ni(II), and Zn(II) from water onto chitosan beads. Adsorption 8, 71–78. http://dx.doi.org/10.1023/A:1015222607996.
Krska, R., Molinelli, A., 2009. Rapid test strips for analysis of mycotoxins in food and feed. Anal. Bioanal. Chem. 393, 67–71. http://dx.doi.org/10.1007/s00216-008-2424-y.
Lagergreen, S., 1898. Zur theorie der sogenannten adsorption gelöster stoffe : Kungliga Svenska Vetenskapsakademiens. 24. Handl., pp. 1–39, pp..
Langmuir, I., 1918. The adsorption of gases on plane surfaces of glass, mica and platinum. J. Am. Chem. Soc. 40, 1361–1403. http://dx.doi.org/10.1021/ja02242a004.
Lerda, D., 2011. Mycotoxin Factsheet. JRC Tech. Notes, 4th edition.
Liu, X.-P., Deng, Y.-J., Jin, X.-Y., Chen, L.-G., Jiang, J.-H., Shen, G.-L., Yu, R.-Q., 2009. Ultrasensitive electrochemical immunosensor for ochratoxin A using gold colloid-mediated hapten immobilization. Anal. Biochem. 389, 63–68. http://dx.doi.org/10.1016/j.ab.2009.03.019.
Ma, D.-L., He, H.-Z., Leung, K.-H., Zhong, H.-J., Chan, D.S.-H., Leung, C.-H., 2013. Label-free luminescent oligonucleotide-based probes. Chem. Soc. Rev. 42, 3427–3440. http://dx.doi.org/10.1039/c2cs35472a.
Monier, M., Ayad, D.M., Wei, Y., Sarhan, A.A., 2010. Adsorption of Cu(II), Co(II), and Ni(II) ions by modified magnetic chitosan chelating resin. J. Hazard. Mater. 177, 962–970. http://dx.doi.org/10.1016/j.jhazmat.2010.01.012.
Morgan, M.R.A., McNerney, R., Chan, H.W.-S., Anderson, P.H., 1986. Ochratoxin a in pig kidney determined by enzyme-linked immunosorbent assay (elisa). J. Sci. Food Agric. 37, 475–480. http://dx.doi.org/10.1002/jsfa.2740370507.
Namasivayam, C., Yamuna, R.T., 1995. Adsorption of direct red 12 B by biogas residual slurry: equilibrium and rate processes. Environ. Pollut. 89, 1–7. http://dx.doi.org/10.1016/0269-7491(94)00056-J.
Nasir, M.Z.M., Pumera, M., 2014. Mycotoxins: simultaneous detection of zearalenone and citrinin by voltammetry on edge plane pyrolytic graphite electrode. Electroanalysis , http://dx.doi.org/10.1002/elan.201400174.
Oztürk, N., Kavak, D., 2005. Adsorption of boron from aqueous solutions using fly ash: batch and column studies. J. Hazard. Mater. 127, 81–88. http://dx.doi.org/10.1016/j.jhazmat.2005.06.026.
Prieto-Simón, B., Campàs, M., Marty, J.-L., Noguer, T., 2008. Novel highly-performing immunosensor-based strategy for ochratoxin A detection in wine samples. Biosens. Bioelectron. 23, 995–1002. http://dx.doi.org/10.1016/j.bios.2007.10.002.
Radi, A.-E., Muñoz-Berbel, X., Cortina-Puig, M., Marty, J.-L., 2009a. An electrochemical immunosensor for ochratoxin A based on immobilization of antibodies on diazonium-functionalized gold electrode. Electrochim. Acta 54, 2180–2184. http://dx.doi.org/10.1016/j.electacta.2008.10.013.
Radi, A.-E., Muñoz-Berbel, X., Lates, V., Marty, J.-L., 2009b. Label-free impedimetric immunosensor for sensitive detection of ochratoxin A. Biosens. Bioelectron. 24, 1888–1892. http://dx.doi.org/10.1016/j.bios.2008.09.021.
Ramakrishna, N., Lacey, J., Candlish, A.A., Smith, J.E., Goodbrand, I.A., 1990. Monoclonal antibody-based enzyme linked immunosorbent assay of aflatoxin B1, T-2 toxin, and ochratoxin A in barley. J. Assoc. Off. Anal. Chem. 73, 71–76.
Ruiz, M., Sastre, A.M., Zikan, M.C., Guibal, E., 2001. Palladium sorption on glutaraldehyde-crosslinked chitosan in fixed-bed systems. J. Appl. Polym. Sci. 81, 153–165. http://dx.doi.org/10.1002/app.1425.
Rusanova, T.Y., Beloglazova, N.V., Goryacheva, I.Y., Lobeau, M., Van Peteghem, C., De Saeger, S., 2009. Non-instrumental immunochemical tests for rapid ochratoxin A detection in red wine. Anal. Chim. Acta 653, 97–102. http://dx.doi.org/10.1016/j.aca.2009.08.036.
Shim, W.-B., Dzantiev, B.B., Eremin, S.A., Chung, D.-H., 2009. One-step simultaneous immunochromatographic strip test for multianalysis of ochratoxin a and zearalenone. J. Microbiol. Biotechnol. 19, 83–92. http://dx.doi.org/10.4014/jmb.0802.105.
Sofie, M., Van Poucke, C., Detavernier, C., Dumoultn, F., Van Velde, M.D.E., Schoeters, E., Van Dyck, S., Averkieva, O., Van Peteghem, C., De Saeger, S., 2010. Occurrence of mycotoxins in feed as analyzed by a multi-mycotoxin LC–MS/MS method. J. Agric. Food Chem. 58, 66–71. http://dx.doi.org/10.1021/jf903859z.
Tessini, C., Mardones, C., von Baer, D., Vega, M., Herlitz, E., Saelzer, R., Silva, J., Torres, O., 2010. Alternatives for sample pre-treatment and HPLC determination of Ochratoxin A in red wine using fluorescence detection. Anal. Chim. Acta 660, 119–126. http://dx.doi.org/10.1016/j.aca.2009.11.011.
Varga, J., Kozakiewicz, Z., 2006. Ochratoxin A in grapes and grape-derived products. Trends Food Sci. Technol. 17, 72–81. http://dx.doi.org/10.1016/j.tifs.2005.10.007.
Visconti, A., Pascale, M., Centonze, G., 1999. Determination of ochratoxin A in wine by means of immunoaffinity column clean-up and high-performance liquid chromatography. J. Chromatogr. A 864, 89–101. http://dx.doi.org/10.1016/S0021-9673(99)00996-6.
Vold, I.M.N., Vårum, K.M., Guibal, E., Smidsrød, O., 2003. Binding of ions to chitosan—selectivity studies. Carbohydr. Polym 54, 471–477. http://dx.doi.org/10.1016/j.carbpol.2003.07.001.
Wan, M.-W., Kan, C.-C., Rogel, B.D., Dalida, M.L.P., 2010. Adsorption of copper (II) and lead (II) ions from aqueous solution on chitosan-coated sand. Carbohydr. Polym. , http://dx.doi.org/10.1016/j.carbpol.2009.12.048.
Yang, J., Kim, S.E., Cho, M., Yoo, I.K., Choe, W.S., Lee, Y., 2014. Highly sensitive and selective determination of bisphenol-A using peptide-modified gold electrode. Biosens Bioelectron, 38–44. http://dx.doi.org/10.1016/j.bios.2014.04.009.
Yu, J., Lai, E., 2010. Molecularly imprinted polymers for ochratoxin A extraction and analysis, Toxins. Basel, pp. 1536–1553. http://dx.doi.org/10.3390/toxins2061536.
Zimmerli, B., Dick, R., 1995. Determination of ochratoxin A at the ppt level in human blood, serum, milk and some foodstuffs by high-performance liquid chromatography with enhanced fluorescence detection and immunoaffinity column cleanup: methodology and Swiss data. J. Chromatogr. B – Biomed. Sci. Appl. 666, 85–99. http://dx.doi.org/10.1016/0378-4347(94)00569-Q.